Supporting information

Recombinase polymerase amplification via proximity hybridization-triggered amplification conversion for detecting diverse nucleic acid targets

Lutan Zhang[a,#], Yuxiao Ma[c,#], Wenbo Wang[a], Jian Zhang[a], Yixi Zhou[a], Yanru Huang[a], Xingmei Yao[a], Lulu Xu[b*], Yunsheng Ge[a*]

[a] Department of Central Laboratory, Women and Children's Hospital, School of Medicine, Xiamen University, Xiamen 361000, China

[b] Department of Laboratory Medicine, Shandong Provincial Hospital Affiliated to Shandong First Medical University, Jinan 250000, China

[c] Department of Cardiology, the First Affiliated Hospital of Xiamen University, School of Medicine, Xiamen University, Xiamen 361000, China

* Corresponding author. E-mail address: gshee@163.com (Y. Ge), cqmuxll@163.com (L. Xu) and 724809959@qq.com (L. Zhang)..

[#] These authors contributed equally to this work.

Reagents and materials

All oligonucleotides were synthesized and HPLC puried by Sangon Biotechnology Co. Ltd. (Zhengzhou, China). The Basic RPA kit was gotten from Suzhou GenDx Biotech Co. Ltd. (Suzhou, China). SYBR Green I was purchased from Solarbio Life Sciences (Beijing, China). All of the sequences are listed in Table S1.

Table S1. Sequences of targets and probes used in this assay.

DNA	Sequence (5'-3')
MTHFR C677T mutation proximity probe a	GTGATGATGAAATCGACTCCCT-C3 spacer-GCCTGCCTGCCTG-C3 spacer-TACTGACTGACTGACTGACT-P
MTHFR C677T mutation proximity probe b	ATCGCATCGCATCGCATCCCAA-C3 spacer-CAGGCAGGCAGGC-C3 spacer-TCAGACACCTTCTCCTTCAAGT-P
wild-type MTHFR gene proximity probe a	GTGATGATGAAATCGGCTCCCT-C3 spacer-GCCTGCCTGCCTG-C3 spacer-TACTGACTGACTGACTGACT-P
wild-type MTHFR gene proximity probe b	ATCGCATCGCATCGCATCCCAA-C3 spacer-CAGGCAGGCAGGC-C3 spacer-TCAGACACCTTCTCCTTCAAGT-P
RPA primer d	AGTCAGTCAGTATTTG
RPA primer e	TCGCATCGCATCGCATCC
Proximity probe a-2	TGATGATGAAATCGACTCCCT-C3 spacer-CCTGCCTGCCTGCCTGCCTG-C3 spacer-TACTGACTGACTGACTGACT-P
Proximity probe a-3	GCGTGATGATGAAATCGACTCCCT-C3 spacer-GCCTGCCTGCCTGCCTG-C3 spacer-TACTGACTGACTGACTGACT-P
Proximity probe a-4	ATGATGAAATCGACTCCCT-C3 spacer-GCCTGCCTGCCTGC-C3 spacer-TACTGACTGACTG-P
Proximity probe b-2	ATCGCATCGCATCGCATCCCAA-C3 spacer-CAGGCAGGCAGGCAGGCAGG-C3 spacer-TCAGACACCTTCTCCTTCA-P
Proximity probe b-3	ATCGCATCGCATCGCATCCCAA-C3 spacer-CAGGCAGGCAGGCAGGC-C3 spacer-TCAGACACCTTCTCCTTCA-P
Proximity probe b-4	ATCGCATCGCATCGCATCCCAA-C3 spacer-GCAGGCAGGCAGGC-C3 spacer-TCAGACACCTTCTCCTTCA-P
RPA primer d-2	AGTCAGTCAGTATTGG
RPA primer d-3	CAGTCAGTAAAATTGG
RPA primer d-4	GTCAGTAAAAAATTGG
RPA primer d-5	CAGTCAGTCAGTATTT
RPA primer d-6	TCAGTCAGTATTTGGG
MTHFR C677T mutation target 1	ACTTGAAGGAGAAGGTGTCTGC-GGGAGTCGATTTCATCATCACGCAGCTTTTC
MTHFR C677T mutation target 2	GAAAAGCTGCGTGATGATGAAA-TCGACTCCCGCAGACACCTTCTCCTTCAAGT
wild-type MTHFR gene target 1	ACTTGAAGGAGAAGGTGTCTGCGG-GAGCCGATTTCATCATCACGCAGCTTTTC
wild-type MTHFR gene target 2	GAAAAGCTGCGTGATGATGAAATC-GGCTCCCGCAGACACCTTCTCCTTCAAGT

SMA proximity probe a ATCGCATCGCATCGCATCCCAA-C3 spacer-
CAGGCAGGCAGGC-C3 spacer-TTGTAAGGAAAATAAAGGAAGA-P
SMA proximity probe b TTTGATTTTGTCTGAAACCT-C3 spacer-
GCCTGCCTGCCTG-C3 spacer-TACTGACTGACTGACTGACT-P
SMN1 exon 7 gene target 1 TTCCTTTATTTTCCTTACAGGGTTTCA-
GACAAAATCAAAAAGAAGGAAGGTGCTCACATT
SMN1 exon 7 gene target 2 AATGTGAGCACCTTCCTTCTTTTTGA
TTTTGTCTGAAACCCTGTAAGGAAAATAAAGGAA

Instruments

Rapid high-throughput, plate-based real-time PCR amplification and detection instruments were carried on CFX Connect Real-Time PCR Detection System (Bio-Rad, USA). The gel electrophoresis and gel image were performed on Horizontal Electrophoresis Systems (Bio-Rad, USA) and Tanon 2500 Imaging System (Tanon Co., Ltd., Shanghai, China), respectively. The genomic DNA was expeditiously extracted by using the Automatic Nucleic Acid Extraction System (DaAn Gene Co., Ltd., Guangzhou, China) and Lab-Aid 824s Nucleic Acid Extraction System (Zeesan Biotech Co., Ltd., Xiamen, China), in strict accordance with the manufacturer's instructions of DNA Extraction and Purification Kit (DaAn Gene Co., Ltd., Guangzhou, China) and Lab-Aid 824s Blood DNA Extraction Kit (Zeesan Biotech Co., Ltd., Xiamen, China). The DNA concentrations were quantified according to the absorption at 260 nm with a NanoDrop One Microvolume UV-Vis Spectrophotometer (Thermo Fisher Scientific, Co., Ltd., Shanghai, China). The detection of MTHFR C677T mutation and SMN1 exon 7 deletion in clinical samples employed mature commercial kits of 5,10-methylenetetrahydro-foiate Reductase Gene 677C/T Polymorphism Assay Kit (Tailored Medical Co., Ltd., Shenzhen, China) and Human Survival Motor Neuron 1 (SMN1) gene Assay Kit (Huizhong Biotech Co., Ltd., Shenzhen, China) respective.

Characterization of target dsDNA at different concentrations by agarose gel electrophoresis

To investigate the band intensity of target dsDNA at different concentrations via agarose gel electrophoresis, we performed serial dilutions of the target dsDNA to

concentrations of 500 nM, 200 nM, 100 nM, 50 nM, 10 nM, and 5 nM, followed by electrophoresis analysis. The results showed that the bands corresponding to the 500 nM (lane 1) and 200 nM (lane 2) target dsDNA were clearly visible with high intensity, whereas no discernible bands were detected for the 100 nM (lane 3), 50 nM (lane 4), 10 nM (lane 5), and 5 nM (lane 6) samples. These observations demonstrate that the agarose gel electrophoresis method lacks the sensitivity to determine target dsDNA at concentrations below 100 nM.

The target concentration of 10 nM was selected for feasibility verification for two reasons. First, 10 nM of target dsDNA was undetectable by gel electrophoresis, which prevented target bands from interfering with the interpretation of other bands. Additionally, the distinct bands of amplification products also demonstrate that our method is feasible for amplifying low-concentration targets.

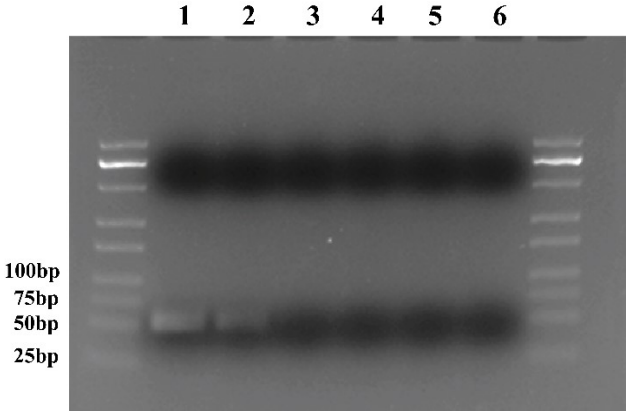

Fig. S1 Characterization of target dsDNA at different concentrations by agarose gel electrophoresis. Lane 1: 500 nM target dsDNA; lane 2: 200 nM target dsDNA; lane 3: 100 nM target dsDNA; lane 4: 50 nM target dsDNA; lane 5: 10 nM target dsDNA; lane 6: 5 nM target dsDNA

The optimal spacer design evaluation

As part of this study, we aimed to determine the optimal spacer length required to minimize nonspecific amplification while maintaining efficient target-specific proximity hybridization. To this end, we evaluated the amplification performance of two spacer lengths (0 nt and 1 nt) in primer d. As shown in Fig. 2B and Fig. S2, shorter spacers (1 nt or 0 nt) in primer d significantly reduced background fluorescence in the RPA reaction. Notably, the 1 nt spacer provided a greater signal

difference between the target and control compared to the 0 nt spacer. This suggests that the 0 nt spacer may impair primer d's binding affinity to proximity probe a due to increased steric interference. In contrast, the 1 nt spacer represents the optimal design, as it effectively suppresses off-target amplification while preserving sufficient hybridization efficiency for target-specific RPA initiation.

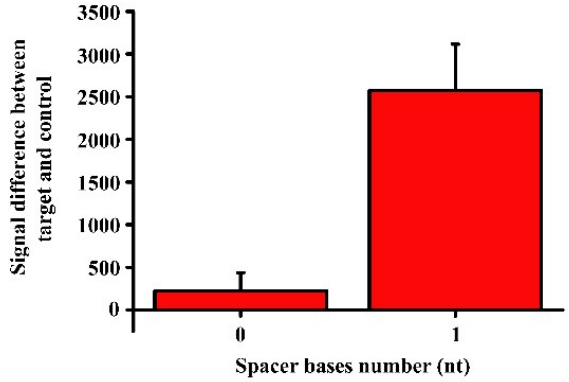

Fig. S2. The signal difference of RPA reaction between the target and control as different primer d with two spacer lengths (0 nt and 1 nt) were added into solution respectively.

Exploration of the optimal number of complementary bases between primer d and proximity probe a.

To determine the optimal number of complementary bases between primer d and proximity probe a, we detected target DNA using primer d variants designed with either 2 or 3 complementary bases. As illustrated in Fig. S3, primer d with 2 complementary bases failed to detect target DNA in our assay, yielding extremely low signals. In contrast, primer d containing 3 complementary bases demonstrated excellent detection performance. These results indicate that 3 complementary bases represent the optimal design for the proposed method.

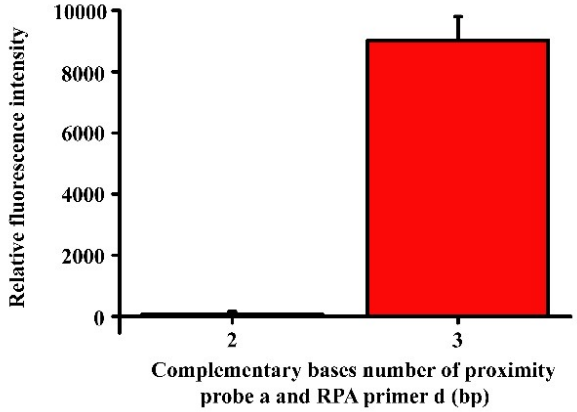

Fig. S3 The fluorescence assay to detect target DNA using primer d variants designed with either 2 or 3 complementary bases.

Optimization of reaction condition in our strategy

To further determine the optimal reaction conditions and enhance the efficiency of our method, key reaction parameters including primer concentration, reaction temperature, and reaction duration were investigated.

First, 1 pM synthetic MTHFR target gene was detected using our strategy at varying primer concentrations (ranging from 50 nM to 600 nM). We found that the method achieved optimal performance when 200 nM primers were employed. Amplification was inhibited at excessively high or low primer concentrations (Fig. S4A). We inferred that low primer concentrations may restrict the strategy's efficiency due to insufficient reaction substrates, whereas excessive primers may inhibit amplification by occupying reaction space.

Second, reactions were performed at different temperatures ranging from 31 °C to 41 °C using our method, and the optimal performance was achieved at 37 °C (Fig. S4B), indicating that enzymatic activity is compromised at excessively high or low temperatures, which impairs amplification efficiency.

Third, we further optimized the reaction duration for our assay. In a series of experiments, we observed that non-specific positive signals began to emerge in blank control reactions when the incubation time was extended to 140 min (Fig. S4C); this non-specific signal is presumably attributable to spontaneous non-specific

hybridization between probes or primer dimer formation induced by prolonged isothermal incubation. As a precaution to eliminate such non-specific interference and ensure high assay specificity, we therefore designated 120 min as the optimal reaction duration.

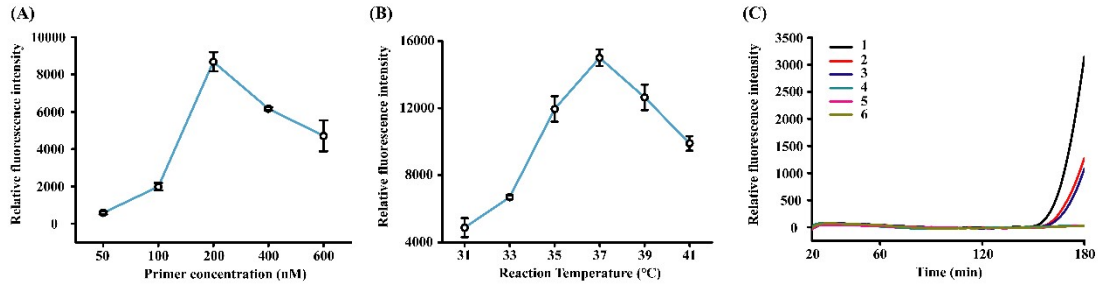

Fig. S4 Optimization of reaction condition include primer concentration (50 nM ~ 600 nM), reaction temperature (31℃ ~ 41℃), and test time (curve 1 to 6 correspond blank 1 to 6).

Verification of robustness and reproducibility

To evaluate the robustness and reproducibility of the proposed method, intra-assay and inter-assay coefficients of variation (CV) were determined using a clinical genomic DNA sample. Two groups were tested, with five parallel replicates in each group. The CV values were all less than 5%, demonstrating satisfactory reproducibility of the method (Figure S5).

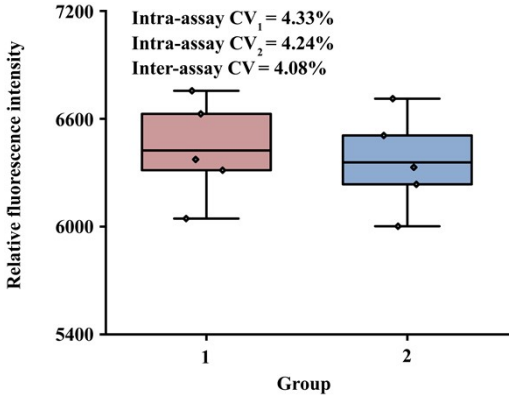

Fig. S5 Intra-assay and inter-assay reproducibility of the proposed method. Intra-assay and inter-assay coefficients of variation (CV) were evaluated using a clinical genomic DNA sample with five parallel replicates in each group.

Detection of the MTHFR C677T mutation in real clinical samples

To further evaluate the clinical applicability and mutation discriminability of our method, we analyzed 50 clinical samples, including 25 with the MTHFR C677T mutation and 25 samples with wild-type target mutation. The test results and detailed information for all 50 clinical specimens are presented in Table 1, Table S2 and Fig. S5. Using our method, all 25 samples with the MTHFR C677T mutation were correctly identified as positive, while all 25 wild-type samples yielded negative results. This demonstrates 100% sensitivity and specificity, confirming the high accuracy and reliability of our approach for detecting MTHFR C677T mutations in clinical settings.

Sample number	P1	P2	P3	P4	P5	P6	P7
Relative fluorescence intensity at the endpoint	7164	6007	7375	9739	4721	15490	11345
Sample number	P8	P9	P10	P11	P12	P13	P14
Relative fluorescence intensity at the endpoint	16566	7184	12440	11382	13146	7326	7845
Sample number	P15	P16	P17	P18	P19	P20	P21
Relative fluorescence intensity at the endpoint	11476	7276	2205	3510	5153	3648	3454
Sample number	P22	P23	P24	P25			
Relative fluorescence intensity at the endpoint	3154	5147	3308	6769			
Sample number	N1	N2	N3	N4	N5	N6	N7
Relative fluorescence intensity at the endpoint	-37.09	-7.21	-15.82	-4.62	-44.76	-28	-38.75
Sample number	N8	N9	N10	N11	N12	N13	N14
Relative fluorescence intensity at the endpoint	86.25	-46.05	-4.62	-56.7	-52.53	-24.47	50
Sample number	N15	N16	N17	N18	N19	N20	N21
Relative fluorescence intensity at the endpoint	-43.81	-22.02	-46.94	-50.93	-45.98	44.18	-17.79
Sample number	N22	N23	N24	N25			
Relative fluorescence intensity at the endpoint	-36.7	-45.47	-52.3	4.88			

Table S2 Endpoint fluorescence data of proposed method for detecting the MTHFR C677T mutation in real clinical samples.

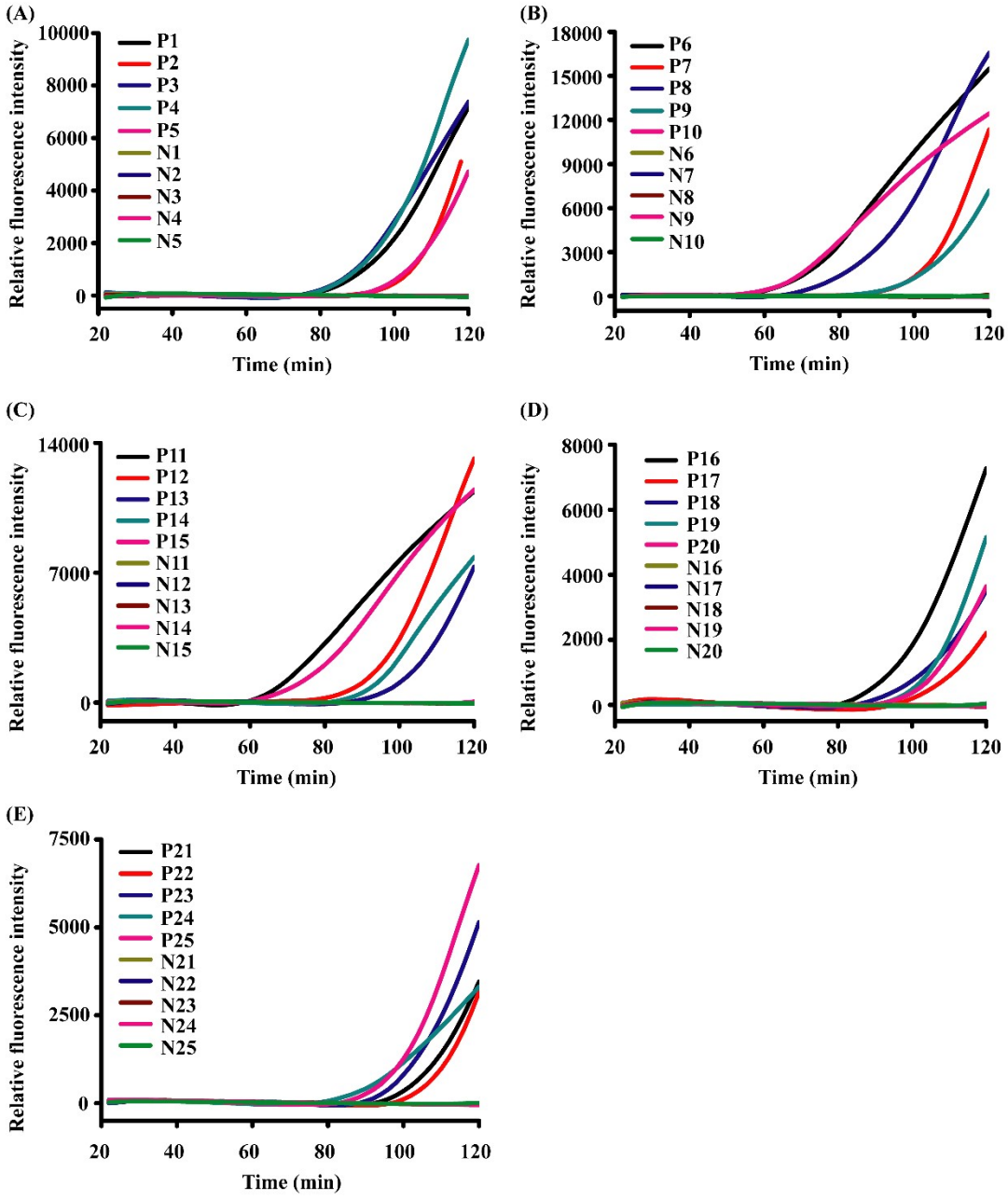

Fig. S6 The real-time fluorescence assay of proposed strategy to detect MTHFR C677T mutation in 50 clinical samples (P1 to P25: the samples with MTHFR C677T mutation, N1 to N25: the samples with wild-type MTHFR C677T mutation).

Detailed data of RT-PCR for detecting the MTHFR C677T mutation in real clinical samples

After the RT-PCR amplification reaction was completed, the detection results

were analyzed by collecting the obtained fluorescence signals. The X-axis was set as the VIC signal (representing genotype C), and the Y-axis was set as the FAM signal (representing genotype T). In the genotyping plot, the samples close to the origin were identified as NTC (No Template Control); those close to the X-axis were interpreted as the CC genotype; and those close to the Y-axis were interpreted as the TT genotype. The detailed clinical detection results (including fluorescence intensity at the endpoint, and qualitative results (positive/negative)) are summarized in Table S3.

Sample number		P1	P2	P3	P4	P5	P6	P7
Relative fluorescence intensity at the endpoint	FAM	584	618	634	643	634	695	672
	VIC	-9.63	-10.7	-9.28	-7.64	-8.88	-12	-10.4
Interpretation results		TT(+)	TT(+)	TT(+)	TT(+)	TT(+)	TT(+)	TT(+)
Sample number		P8	P9	P10	P11	P12	P13	P14
Relative fluorescence intensity at the endpoint	FAM	580	596	821	648	459	471	503
	VIC	-12.1	-12.4	-7.96	-12.1	-4.12	-0.941	-4.56
Interpretation results		TT(+)	TT(+)	TT(+)	TT(+)	TT(+)	TT(+)	TT(+)
Sample number		P15	P16	P17	P18	P19	P20	P21
Relative fluorescence intensity at the endpoint	FAM	459	669	472	811	718	763	760
	VIC	-5.35	-9.37	-8.26	-7.97	-9.06	-12.7	-6.24
Interpretation results		TT(+)	TT(+)	TT(+)	TT(+)	TT(+)	TT(+)	TT(+)
Sample number		P22	P23	P24	P25			
Relative fluorescence intensity at the endpoint	FAM	733	759	746	718			
	VIC	-11.0	-8.1	-8.12	-5.32			
Interpretation results		TT(+)	TT(+)	TT(+)	TT(+)			
Sample number		N1	N2	N3	N4	N5	N6	N7
Relative fluorescence intensity at the endpoint	FAM	-5.83	-5.57	-4.93	-3.67	-4.45	-8.79	-6.29
	VIC	1581	1835	1764	1623	1759	1576	1542

Interpretation results		CC(-)	CC(-)	CC(-)	CC(-)	CC(-)	CC(-)	CC(-)
Sample number		N8	N9	N10	N11	N12	N13	N14
Relative fluorescence intensity at the endpoint	FAM	-4.70	-4.77	-3.68	-5.03	-4.51	-4.22	-6.50
	VIC	1486	1599	1465	1585	1614	1544	1602
Interpretation results		CC(-)	CC(-)	CC(-)	CC(-)	CC(-)	CC(-)	CC(-)
Sample number		N15	N16	N17	N18	N19	N20	N21
Relative fluorescence intensity at the endpoint	FAM	-4.69	-4.43	-4.78	-6.72	-5.71	-4.85	-3.94
	VIC	1945	1565	1547	1738	1766	1522	1602
Interpretation results		CC(-)	CC(-)	CC(-)	CC(-)	CC(-)	CC(-)	CC(-)
Sample number		N22	N23	N24	N25			
Relative fluorescence intensity at the endpoint	FAM	-3.13	-4.45	-4.97	-4.67			
	VIC	1778	1753	1702	1618			
Interpretation results		CC(-)	CC(-)	CC(-)	CC(-)			

Table S3 Detailed data of RT-PCR for detecting the MTHFR C677T mutation in real clinical samples.

Comparative analysis of the detection results using the same batch of clinical samples extracted with two different commercial DNA extraction kits

To further demonstrate the robustness and practical applicability of our assay in clinical settings, we have conducted a comparative analysis of the detection results using the same batch of clinical samples (3 mutant-type samples and 3 wild-type samples) extracted with Lab-Aid 824s Blood DNA Extraction Kit (Zeesan Biotech Co., Ltd., Xiamen, China) and DNA Extraction and Purification Kit (DaAn Gene Co., Ltd., Guangzhou, China). The results showed that the endpoint values (120 min) and positive detection rates of the target mutation (MTHFR C677T) were highly consistent across the two groups (Fig. S6). This comparative data confirms that our assay exhibits excellent compatibility with various commonly used commercial DNA

extraction kits, and its performance remains stable even when different sample purification workflows are applied. Such compatibility is of great practical significance for clinical laboratories that may adopt different DNA extraction systems, further supporting the potential of our assay for routine clinical application.

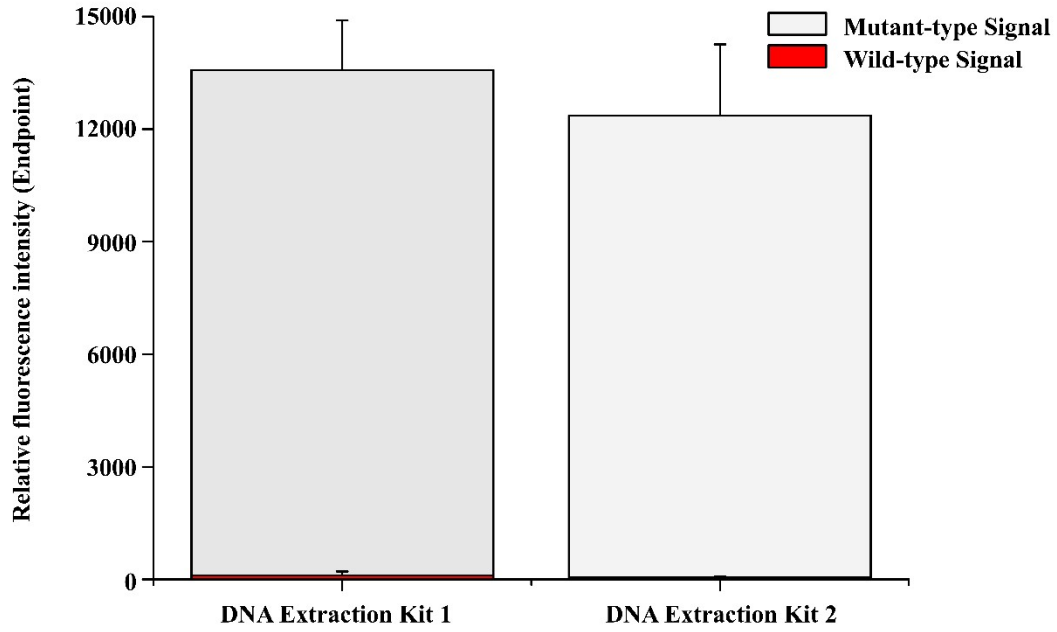

Fig. S7 Comparative analysis of the detection results using six clinical samples extracted with two different commercial DNA extraction kits, including DNA extraction kit 1 (Lab-Aid 824s Blood DNA Extraction Kit from Zeesam biotech Co., Ltd.) and DNA extraction kit 2 (DNA Extraction and Purification Kit from daan gene Co., Ltd.).

The cost calculation of our method for clinical samples detection

The cost calculation is based on the bulk purchasing prices of reagents and consumables, as well as the average depreciation and electricity cost of the instruments used (real-time fluorescence detection platform).

Cost Component	Cost per test
RPA kit (including enzymes, buffers, etc.)	~$4.00
DNA primers (all oligonucleotides used in the assay)	~$0.20

Fluorescent dye (SYBR Green I)	~$0.05
Experimental consumables (e.g., reaction tubes, pipette tips)	~$0.15
Instrument usage cost (including electricity fee for isothermal incubation and fluorescence detection)	~$0.60
Total	~$5.00

Table S4 The cost calculation of our method for per clinical samples detection

SMN1 exon 7 deletion analysis in clinical samples

To further evaluate the clinical applicability of our methodology for deletion detection, we analyzed 12 clinical samples comprising: two with homozygous SMN1 exon 7 deletions, six with heterozygous SMN1 exon 7 deletions, and four normal control samples. Fluorescence assay results for all samples are presented in Fig. S7 and Table S5. Using our proposed method, we successfully identified the two homozygous deletion samples as negative, while four normal controls tested positive. The heterozygous deletion cases were correctly classified as weak positive. These results demonstrate the high accuracy and clinical feasibility of our approach for detecting deletion variants.

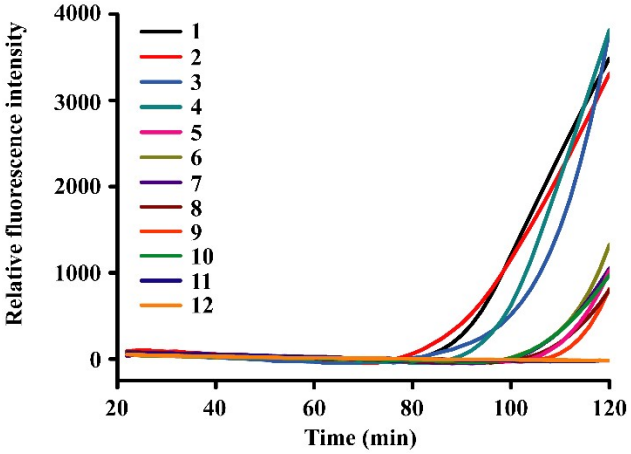

Fig. S8 The real-time RNA assay of 12 samples for SMA screening. 12 clinical samples comprising: two with homozygous SMN1 exon 7 deletions (curve 11 to 12), six with heterozygous SMN1 exon 7 deletions (curve 5 to 10), and four normal control samples (curve 1 to 4).

Sample number	1	2	3	4	5	6	7
Relative fluorescence intensity at the endpoint	3486	3308	3803	3814	813	1324	1050
Interpretation results	normal	normal	normal	normal	heterozygous	heterozygous	heterozygous
Sample number	8	9	10	11	12		
Relative fluorescence intensity at the endpoint	802	1021	971	-18.42	-16.13		
Interpretation results	heterozygous	heterozygous	heterozygous	homozygous	homozygous		

Table S5 Endpoint fluorescence data of proposed method for detecting the SMN1 Exo 7 deletion in real clinical samples.

Detailed data of RT-PCR for detecting the MTHFR C677T mutation in real clinical samples

After the RT-PCR amplification reaction was completed, the detection results were analyzed by collecting the obtained fluorescence signals (Table S6). The SMN1 gene (target gene) was detected using a VIC-labeled probe, while the β-actin gene (reference gene) was detected using a CY5-labeled probe, with ROX serving as the reference fluorescence. The copy number of the SMN1 gene in the samples was calculated using the following formulas: (1) $\Delta Ct_{(\text{test sample / control sample})} = Ct_{(\text{target gene})} - Ct_{(\text{reference gene})}$; (2) $\Delta\Delta Ct_{(\text{test sample})} = \Delta Ct_{(\text{test sample})} - \Delta Ct_{(\text{control sample})}$; (3) RQ value (Expression value)$_{(\text{test sample})} = 2^{-\Delta\Delta Ct}$

The reference interval was established using clinical samples, and the criteria are defined as follows: (1) 0 copy of the gene: RQ value (Expression value) < 0.25 or no RQ value (Expression value) detected; (2) 1 copy of the gene: RQ value (Expression value) = 0.25-0.75; (3) 2 copies of the gene: RQ value (Expression value) = 0.75–1.25.

Sample number	1	2	3	4	5	6	7

Relative fluorescence intensity at the endpoint	Vic	2246	2407	2227	2270	1824	1884	1535
	Cy5	1659	1814	1778	1846	1849	1815	2367
Interpretation results		normal	normal	normal	normal	heterozygous	heterozygous	heterozygous
Sample number		8	9	10	11	12		
Relative fluorescence intensity at the endpoint	Vic	1442	1566	1812	414	316		
	Cy5	1849	1708	1472	1876	1481		
Interpretation results		heterozygous	heterozygous	heterozygous	homozygous	homozygous		

Table S6 Endpoint fluorescence data of RT-PCR for detecting the SMN1 Exo 7 deletion in real clinical samples.

Systematical comparation between our method and other RPA-integrated nucleic acid detection strategies

We systematically compare our proposed method with other RPA-integrated and isothermal amplification nucleic acid detection strategies reported in recent studies (Table S7). Key points of the comparison are summarized as follows:

In terms of multi-target-detection applicability, our method highlights by enabling the detection of three distinct target types (wild-type genes, single-base mutations, and exon deletions), whereas all other RPA-based or isothermal amplification methods included in the comparison are limited to detecting a single target type.

Regarding the limit of detection (LOD), although the LODs of other RPA methods are also impressive, direct horizontal comparison is not feasible due to inconsistent expression formats (such as concentration and abundance) across different studies.

For detection time, our method requires 120 minutes, which is slightly longer than the 60 minutes of most other RPA methods. This compromise is attributable to the mechanism design necessary to achieve multi-target-type detection specificity.

Notably, this duration is still shorter than the general detection time of conventional RT-PCR methods, thus maintaining the method's practical advantages.

Therefore, this comparison further highlights the multi-target-detection applicability of our strategy.

Methodology	Amplification principle	Target type	Steps	LOD	Sensitivity	Specificity	Test time
RPA-Cas12a [21]	PAM-dependent Target-dependent	Streptomycin-resistant mutations	Two-steps	0.1%	100%	100%	60 min
Blocked-RPA [22]	Target-dependent	KRAS gene	Two-steps	4ng	-	-	60 min
AS-RPA [6]	Target-dependent	β^A globin and β^S globin alleles	One-step	100 copies	100%	94.7% /97.1%	30 min
Microfluidic RPA-Cas12a [23]	Target-dependent PAM-dependent	HPV DNA	Two-steps	0.26aM	97.8%	98.1%	40 min
RPA-Cas12a/13a [24]	PAM-dependent Target-dependent	SARS-CoV-2 and African Swine fever virus	One-step	40 copies	100%	100%	30 min
Asymmetric RPA [25]	Target-dependent	SNP	Two-steps	100pM	-	-	60 min
RPA-Cas12a [26]	Target-dependent PAM-dependent	SMN1 gene	One-step	1.8 pM	100%	100%	60 min
LAMP [27]	Target-dependent	p.E746-A750del	One-step	30 copies			30 min

PA-LAMP [28]	Target-dependent	Kras gene	One-step	22 aM			100 min
RCA-FRET [29]	Target-dependent	BRAF gene	Two-steps	4.5x10^{5} copies			270 min
DNAzyme-activated RCA [30]	Target-dependent	rpoB 531	One-step	0.3 fM			100 min
Our method	Amplification conversion	MTHFR gene, MTHFR C677T mutation, and SMN1 exon 7 deletion	One-step	0.1ng	100%	100%	120 min

Table S7 Systematical comparation between our method and other RPA-integrated and isothermal nucleic acid detection strategies.